Bachelor's Thesis

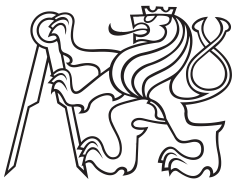

Czech Technical University in Prague

F3

Faculty of Electrical Engineering
Department of Cybernetics

Unmanned Aerial Vehicle Design and Sensor Integration for Flying over Water Area

Ivan Čermák

Supervisor: Ing. Pavel Stoudek
May 2022

BACHELOR‘S THESIS ASSIGNMENT

I. Personal and study details

Student's name: **Čermák Ivan** Personal ID number: **492058**

Faculty / Institute: **Faculty of Electrical Engineering**

Department / Institute: **Department of Cybernetics**

Study program: **Cybernetics and Robotics**

II. Bachelor’s thesis details

Bachelor’s thesis title in English:

Unmanned Aerial Vehicle Design and Sensor Integration for Flying over Water Area

Bachelor’s thesis title in Czech:

Návrh bezpilotního letounu a integrace senzorů pro létání nad vodní plochou

Guidelines:

This thesis aims to design an Unmanned Aerial Vehicle (UAV) for outdoor flying above water areas. The UAV will be equipped with sensors required for an autonomous flight and for a detection of a water surface. Moreover, the UAV will be water resistant and able to land on water.
1. Design the mechanical solution
a. Use the T650 drone kit.
b. Explore the possibilities of protection against water (mechanical, chemical, etc.).
c. Design a landing gear for the events of water landing.
2. Explore the sensory solution for the detection of a water surface and integrate it with the designed platform.
3. Implement a program for the onboard computer of the UAV to acquire data for the sensor comparison. This program must be implemented using ROS for the use with the MRS group system.
4. Perform the practical experiment if possible (depends on the MRS group schedule and other circumstances).
5. Present and discuss the results.

Bibliography / sources:

[1] Y. Bai, et al. "Development of a Novel Water Landing UAV with Deflatable Floater," 2019
[2] H. Niu, et al. "Design, Integration and Sea Trials of 3D Printed Unmanned Aerial Vehicle and Unmanned Surface Vehicle for Cooperative Missions," 2021
[3] Y. H. Tan, et al. "A Lightweight Waterproof Casing for an Aquatic UAV using Rapid Prototyping," 2020
[4] Anis Koubaa, Robot Operating System (ROS), The Complete Reference (Volume 3), 2018
[5] Báča, Tomáš, et al. "The MRS UAV System: Pushing the Frontiers of Reproducible Research, Real-world Deployment, and Education with Autonomous Unmanned Aerial Vehicles", 2021

Name and workplace of bachelor’s thesis supervisor:

Ing. Pavel Stoudek Multi-robot Systems FEE

Name and workplace of second bachelor’s thesis supervisor or consultant:

Date of bachelor’s thesis assignment: **21.01.2022** Deadline for bachelor thesis submission: **20.05.2022**

Assignment valid until: **30.09.2023**

Ing. Pavel Stoudek	prof. Ing. Tomáš Svoboda, Ph.D.	prof. Mgr. Petr Páta, Ph.D.
Supervisor’s signature	Head of department’s signature	Dean’s signature

III. Assignment receipt

The student acknowledges that the bachelor's thesis is an individual work. The student must produce his thesis without the assistance of others, with the exception of provided consultations. Within the bachelor's thesis, the author must state the names of consultants and include a list of references.

. _____ Date of assignment receipt

_____ Student's signature

Acknowledgements

I would like to thank Ing. Pavel Stoudek for his guidance, Bc. Ondřej Procházka and Bc. Filip Novák for their tips on MRS Experimental Camp, Bc. Tomáš Musil, who encouraged me to do my thesis in the MRS team, Bc. Lev Kisselyov and my family for supporting me during my studies and finally doc. Ing. Martin Saska, Dr. rer. nat. for giving me this opportunity.

Declaration

I declare that the presented work was developed independently and that I have listed all sources of information used within it in accordance with the methodical instructions for observing the ethical principles in the preparation of university theses.

Prague, May, 2022

Prohlašuji, že jsem předloženou práci vypracoval samostatně a že jsem uvedl veškeré použité informační zdroje v souladu s Metodickým pokynem o dodržování etických principů při přípravě vysokoškolských závěrečných prací.

Abstract

Unmanned Aerial Vehicles (UAVs) are used for many tasks in various environments. The flight above water surface is one of the more challenging.

The drone is required to withstand contact with water and be equipped with suitable landing gear in the case of emergency water landing. The hardware design must address these problems. Moreover, the sensory equipment must be carefully chosen for reliable detection of the water surface.

In the beginning, the thesis provides an overview of currently used solutions utilizing various Unmanned Vehicles. Based on the review, a Tarot T650 drone equipped with a water-resistant cover and water landing gear is developed. Firstly, the possibilities of protection against water are explored. Secondly the water landing gear is designed and lastly, the suitable sensory equipment is chosen and mounted on the platform.

With the hardware solution complete, a ROS node is created to integrate the sensors with the Multi-robot Systems group (MRS) system. Finally, the UAV platform is thoroughly tested during the MRS experimental campaign.

Keywords: UAV, Unmanned aerial vehicle, Water-resistant, Drone, Floating gear, Flying above water

Supervisor: Ing. Pavel Stoudek

Abstrakt

Bezpilotní multirotorové helikoptéry (drony) se používají k mnoha účelům v různých prostředích a proměnlivých podmínkách. Let nad vodní hladinou patří mezi více náročné úlohy.

Je důležité, aby byla řídící elektronika bezpilotní helikoptéry dostatečně chráněná proti přístupu vody. Dron také musí být vybaven plováky v případě nouzového přistání na vodě. V neposlední řadě je třeba vhodně zvolit senzory pro přesnou detekci vodní hladiny.

Nejprve je představen současný stav využití různých bezpilotních helikoptér určených pro lety nad vodní plochou. Na základě této rešerše je navržen dron Tarot T650 vybavený voděodolným krytem a plováky. Jsou zmíněny možnosti ochrany proti přístupu vody, dále návrh plováků a nakonec jsou vybrány vhodné senzory.

Pro integraci senzorů se systémem Multi-robotické skupiny (MRS) je vytvořen program s využitím ROS. Na závěr je platforma otestována během experimentální kampaně MRS v Temešváru u Písku.

Klíčová slova: UAV, Bezpilotní helikoptéra, Voděodolný, Dron, Plováky, Let nad vodou

Překlad názvu: Návrh bezpilotního letounu a integrace senzorů pro létání nad vodní plochou

Contents

Chapter 1

Introduction

The field of Unmanned Aerial Vehicles (UAVs) or drones is an attractive topic with many applications. Drones have many uses - in both military and civilian areas. They can be used to deliver goods, collect samples or explore dangerous or inaccessible places. For this reason, many research teams and companies strive to improve the state of the art in the world of drones.

The Multi-robot Systems group at Department of Cybernetics, Faculty of Electrical Engineering, CTU in Prague is a research group, which specialises in autonomous drones, trajectory planning, drone swarms and exploration. So far, there have not been many experiments concerning drones and water. Even a few water drops from a light shower can interrupt any experiment the group is conducting at the moment. The group has no drones optimised for water encounters and having such drone will bring new opportunities to the MRS group. In this thesis, the Tarot T650 drone will be modified to be water resistant, be able to fly in close proximity of water and be able to determine how close to the surface it is flying at the moment. This drone was selected, because the MRS group has a lot of experience with this type of drone platform.

1.1 Goals

The goal of this thesis is to design a drone based on the Tarot T650 platform, which is able to:

- Detect water surface and measure its distance from the surface
- Safely float on the water surface
- Comply to certain IP standard

1.2 Organisation of the thesis

In chapter 2, water-resistivity is defined and related drone projects are presented. In chapter 3, the drone is introduced and described. Chapter 4 is divided into two sections, which describe the two main methods of achieving water-resistivity. In chapter 5, the solution for flotation is described. In chapter 6, various sensory options are explored and the best sensor is selected and chapter 7 is centered on integrating the sensor into the MRS UAV system. Chapter 8 is dedicated to experimental verification of the proposed designs. Each of chapters 4, 5 and 7 covers one topic of the goals. Chapter 9 concludes this thesis and in chapter 10 the results are discussed and possible future work is mentioned.

Chapter 2
Related work

In this section, water-resistivity is defined and related solutions are presented, both scientific and commercial. Mentioned scientific drones are mostly in the prototype stage and are often adaptable to new tasks, whereas the commercial ones are usually single-purpose.

2.1 Water-resistivity

Some products, especially electronic goods, can be susceptible to damage from water. The damage can range from cosmetic discoloration, signal distortion, to fatal short-circuit and total destruction. When circuits are left unprotected and come into contact with water, new conductive paths are introduced in the circuit, which are the reason why damage occurs.

Pure, deionised water is not a good conductor. When measured, its electrical resistance is approximately 18.2 $M\Omega cm^{-1}$ [1]. However, water in this state is not present anywhere in the world, as there are always some impurities dissolved. Electric resistance of tap water in Prague was measured to be 3223 Ωcm^{-1}. The electric resistance of seawater is 5.5 $S \cdot m^{-1}$, which is approximately 0.18 Ωm^{-1} [2].

Water-resistivity is the ability of products which determines, what conditions the products can survive unaffected. These conditions were specified in IEC 60529[3], where protection categories against both solid object and liquid damage are stated. This article is the basis for the publicly known IP standard. The first digit states, how resilient is the product to solid particles and items. For example, IP2X certification states, that a standardised finger-shaped tool will not damage the product and the person touching it. The categories concerning water protection are divided into 10 ranks, where higher number means higher resistance. When the letter X is used in specification, it means, that the category, where the letter is placed, was not tested or is irrelevant to a statement, which is being made about the product. The second digit specifies, how rugged the product is concerning water contact. IPX0 states, the product was not designed with any ruggedness in mind. IPX4 certification tells the user, that the product will withstand splashes of water from any direction. IPX9 certificate is often required for critical medical hardware, for it must withstand high-pressure cleaning. As a side note, medical electronics

also it must withstand chemical disinfectants but those are not considered in the IP standard.

2.2 Scientific drones

Marine drones have their place in the scientific world. Some projects are more application-oriented, where drones collect data in inaccessible environments, or speed up the process. For example, a water sampling drone was created by Daniel Štanc in [4] in his bachelor's thesis. The drone is able to collect 4 samples in separate containers, while also being able to prevent cross-contamination. However, no steps were taken to make the drone water-resistant and in the case of an emergency, the drone would possibly get damaged by water.

Hardware-oriented articles are more concerned with the process of building a drone than its application. Bai Yiyun et. al. in [5] developed a drone with inflatable floaters, which is able to float on the surface of water, however, the final product is not shown in the article. H. Niu et. al. in [6] developed a combination of a USV and a UAV for cooperative missions. The USV acts as a mobile base and the UAV carries out tasks. The water-resistivity of the UAV was not discussed.

Yu Herng Tan et. al. in [7] designed and built a completely waterproof hybrid drone, which is able to fly above water and also swim in the water. The main waterproofing element was a plastic shell, which prevented the water from making contact with electronics. The authors concentrated on making the whole project using 3D printers. When generalised, the final design consisted of a shell with a few compartments, which were closed in a watertight manner utilising gaskets printed from flexible and deformable thermoplastic polyurethane(TPU).

Figure 2.1: Drone of Yu Herng Tan et.al. in [7]

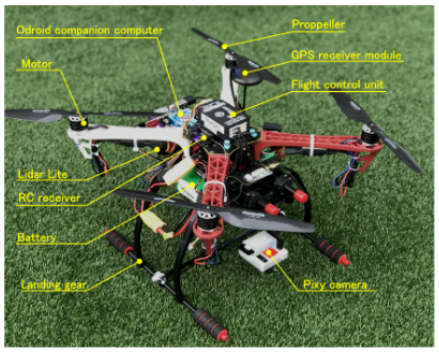

Figure 2.2: Drone of Xuan-Mung, N. et. al in [8]

2.3 Commercial drones

From the commercial point of view, water-resistant drones are intriguing, because they enable their users to operate them in harsher conditions or environments. For example, delivery drones capable of flight in the rain can increase the amount of successful deliveries, thus offering the company a competitive advantage. However, not many companies offer drone deliveries to this date.

Another marketable specialisation of marine drones are cinematography marine drones. Capturing drone shots in near vicinity or filming drones made for free-style flight near water requires perfectly waterproof drones. These drones are often single-purpose and do not offer much customisation. Their bodies are rigid, waterproof and ensure the buoyancy needed for the drone to float on the water.

Finally, drones which assist with fishing are also on the market. This category offers a camera paired together with a simple robotic gripper fixed to the body of the drone. The combination allows the user to drop fishing bait with high accuracy, which is used by some fishing enthusiasts[9].

Name	Weight[kg]	Flight time[min]	Range[m]	Price[USD]
QuadH2O	-	10	-	850
Spry+	2.18	15	800	1000
SplashDrone 3	2.18	25	5000	2500

Table 2.1: Commercially available filming drones

Figure 2.3: SwellPro Splashdrone 3 [10]

Figure 2.4: SwellPro Spry+ [11]

Chapter 3

Drone description

3.1 Base kit

The base for the hardware platform used for the experimental part of this thesis is the Tarot 650 drone kit, which implements a standard four-motor quadrocopter configuration. Technical specifications can be seen in table 3.2 and technical drawing can be seen in the picture 3.1, as it is stated in [12].

Part	Name	note [-]
Motor	Tarot 4114/320KV	outrunner brushless DC motor with 22 poles
Battery	TATTU	6S LiPo battery with 8000mAh capacity at 22.2V
Carbon parts	-	body parts of the frame of the drone
Autopilot	Pixhawk	Flight controller with *Ardupilot* firmware
ESCs	Turnigy MultiStar	Capable of delivering up to 51A

Table 3.1: Tarot 650 kit parts

The dimensions of the unmodified drone can be seen in the picture 3.1.

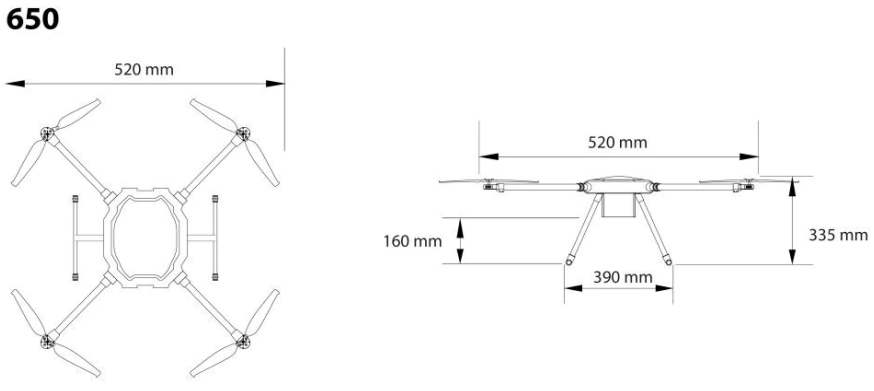

.

Figure 3.1: Technical drawing of the Tarot T650 drone from [12]

3.2 MRS modifications

The Tarot 650 is a multi-functional platform, which allows the end user to tailor the drone for a specific task. The following components are frequently used:

Part	Name	Note
Firmware	-	Custom MRS Firmware based on `PX4`
Computer	`Intel NUC`	computer with `Intel i7`, on which the `MRS UAV` system runs
RGBD camera	`Intel RealSense F435`	Used for gathering visual data or for input to controllers
Height sensor	`Garmin LIDAR-LiteV3`	Near-infrared time-of-flight distance sensor
LIDAR	`RpLidar A3`	Near-infrared time-of-flight 1-row lidar
LIDAR	`Ouster OS0`	Near-infrared time-of-flight 128-row lidar
RTK	`REACH M2`	GPS receiver and system for increasing the localisation accuracy

Table 3.2: MRS additions to Tarot 650

Chapter 4

Protection against water

Each component of the drone has specific waterproofing needs, but in general, a barrier, impermeable by water molecules must be created. The barrier can be an enclosure, a layer of lacquer or generally a protective film. The simplest way of protecting sensitive components is to put them inside a case, which will completely enclose these components. In this section, both approaches are considered and discussed.

4.1 Shell

Completely enclosing the internal electronics of the drone is possible, but beyond the scope of this work. The most problematic component is the Intel NUC computer, which needs active cooling via airflow. Therefore, the whole shell consists of three components:

- Main shell
- Secondary shell
- Air ducts

4.1.1 Prototyping

Three materials, popular for drone-making and in RC-hobby world, were considered - 3D printable plastic, balsa wood and carbon fibre. Carbon fibre, despite being mechanically superior, was ruled out, because it is not as easily modifiable and cheap as plastic. Another factor was, that the manufacturing period is too long for prototype-making. Balsa wood was also rejected for being too difficult to work with for beginners. With the advantage of fast prototyping in mind, the protective shell was 3D printed from PETG material. This filament was used to print the shell because it can produce strong parts and has a relatively low shrinkage ratio compared to other filament types.

As a base shape, a box with octagonal base was chosen. This shape is more durable and aerodynamic than a rectangular box and also provides flat surfaces, which are good for mounting other objects or for passing wires inside the shell. The shell was designed in closed-source, cloud-based, commercial Fusion360 CAD software, developed by Autodesk Software.

The shell is affixed to the topmost body plate via a pattern of matching fixings, standard M3 fasteners were used for easy assembly and disassembly. The top and bottom part are held together by screws and also there is a groove on the top and a lip on the bottom part. the groove can be filled with a gasket or a silicone insulation paste.

Secondary shell. In order to sense the world, drones need data from sensors. Many sensors use wires to transport data to the onboard computer, and a water-resistant way of implementing this way of communication is needed. Therefore, an extension of the shell was created, in a very similar manner as the original one. It is similarly divided into two bodies - top and bottom part, but there are eight semi-circle cut-outs on both parts, which fit together and form small circular holes in the secondary shell. The cut-outs are filled with easily deformable silicone caulk *Dowsil* and the silicone is left to cure, while the mini-shell is left open, otherwise the curing caulk would and „glue“ the parts of the secondary shell together. After curing, the caulk is able to wrap itself around the signal cables and creates a waterproof seal. If the caulk deformability decreases, it can be scraped out and replaced with fresh, pliable caulk. The location for the secondary shell was chosen to be at the top of the main shell body. This approach forces the user to route the cables to sensors one specific way, which is far enough from propellers.

Air ducts. As the onboard computer requires active air cooling, ducts for air need to be made. Such duct must not be a considerable obstacle for airflow, must be heat resistant and should prevent easy water ingress. The proposed designs can be seen in the picture 4.6.

Each air duct is split into two physical bodies, the bottom and top one. The common edge is designed in such a way, that the top and bottom part fit together and are held by friction. The bottom one will be glued to the bottom part of the shell and the top will remain removable to allow access to USB ports of the NUC.

The air ducts were tested to be able to withstand the hot exhaust from the computer. The computer ran a stress-test for 30 minutes, when every core and thread was under 100% load and core temperature and clock frequency was measured. The program `s-tui monitor` was used for testing[13]. One test was carried out as a reference, without any modification of the cooling system. One test was carried out with the intake and exhaust ducts in place. The temperature and clock frequency was measured to be the same in both cases, approximately 75°C and 3.4GHz.

The IP rating is estimated for the drone and electronics mounted inside the shell. The main risk for water ingress pose the air ducts. As the openings are pointed downwards and the drone is flown with horizontal stabilisation, the drone should pass the following tests:

- IPX1 - water dripping perpendicular from above the drone
- IPX2 - water dripping from above the drone, which is tilted ± 15°

- IPX3 - water dripping from above the drone, which is tilted ± 60°

The IPX4 test consists of relatively weak water jets being sprayed on the drone from all angles. As the air flowing through the ducts makes three 90° turns and it is estimated, that no water droplets will be able to traverse through. In addition, the flow of air through the air ducts is not intense enough to carry water droplets.

4.1.2 Proposed solution

The final version was made 1 centimetre taller and 2 centimetres wider, to better accommodate cables and air ducts. Furthermore, the design of the shell was rotated 90°.

In standard MRS usage, the whole power system is soldered together. The power system of the drone comprises of the battery, which is connected to the power delivery board(PDB), which is mounted on the carbon body plate. The ESCs, which are connected to the PDB, are located on the carbon arms below the motors. This way, only two DC power wires and two signal wires carrying digital communication go through each carbon arm. During the work on this thesis, another design was implemented and tested, which moves the ESCs to a different place - inside the shell - and removable connectors are affixed to the walls of the shell. From there, wires go around the shell, enter the carbon tubes and then connect to the motors. The aim of this design is to make the power system together with the shell more modular, so that the wires connected to the motors are not embedded in the shell, which is supposed to make the assembly and disassembly of the drone easier.

The whole drone can be seen in the picture 4.8, a detailed view on the shell is in the picture 4.6, the secondary shell is depicted in pictures 4.1 and 4.2 and a detailed view on the flotation devices is in pictures 4.3 and 4.4. The file is one of the attachments to this thesis.

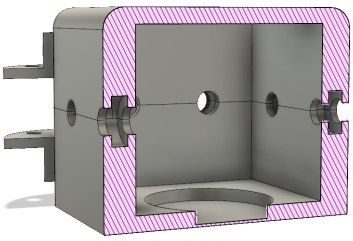

Figure 4.1: 3D model of the secondary shell.

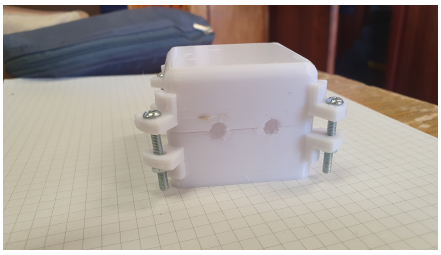

Figure 4.2: Finished secondary shell.

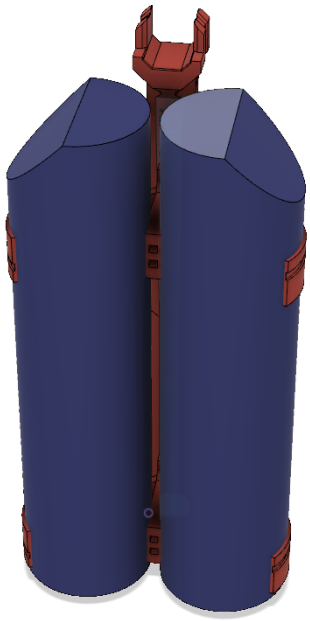

Figure 4.3: 3D model of the floater.

Figure 4.4: Finished floater.

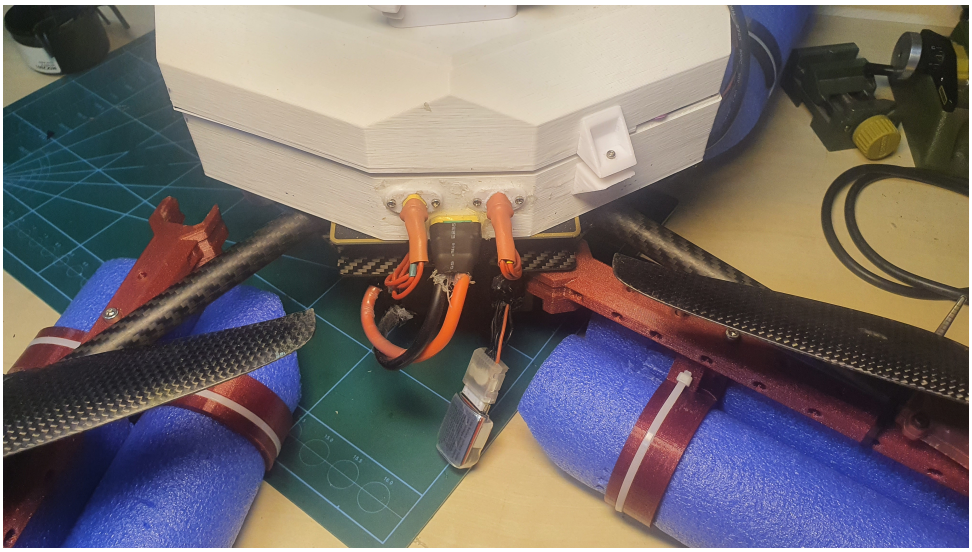

Figure 4.5: The newly implemented motor connection design.

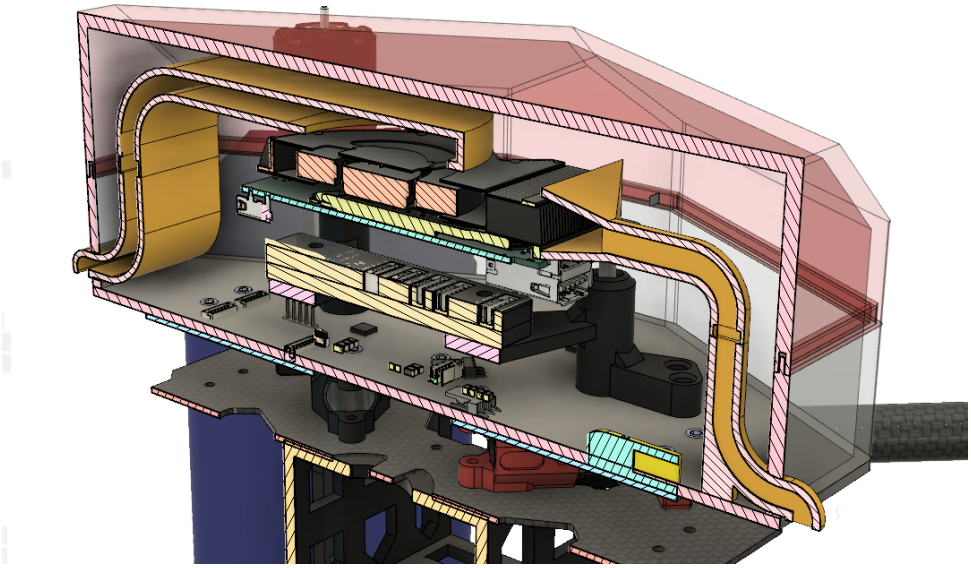

Figure 4.6: A detailed view on the air ducts.

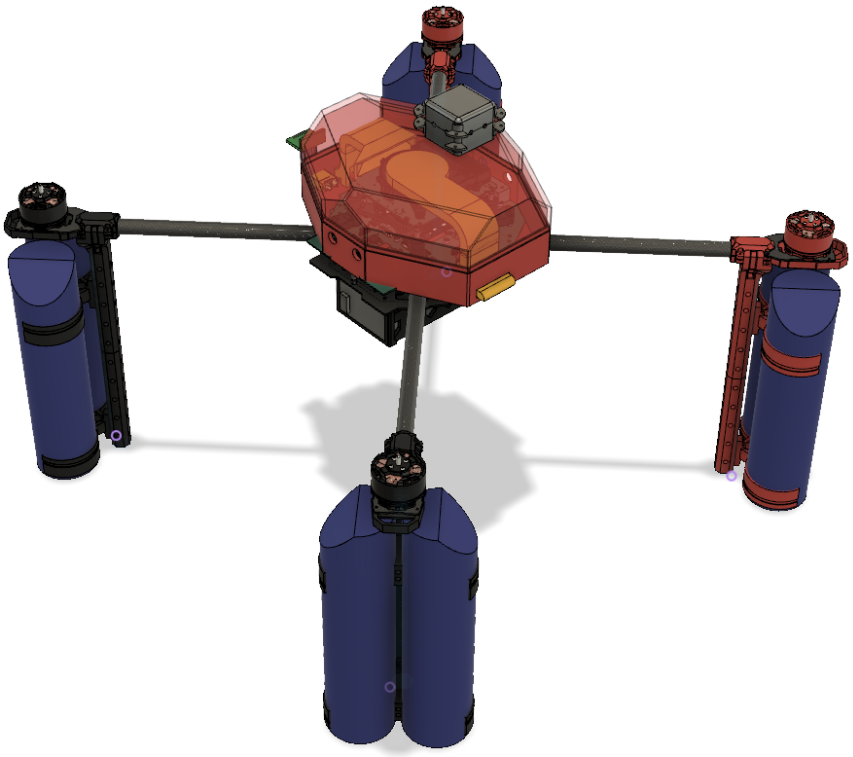

Figure 4.7: Complete drone design.

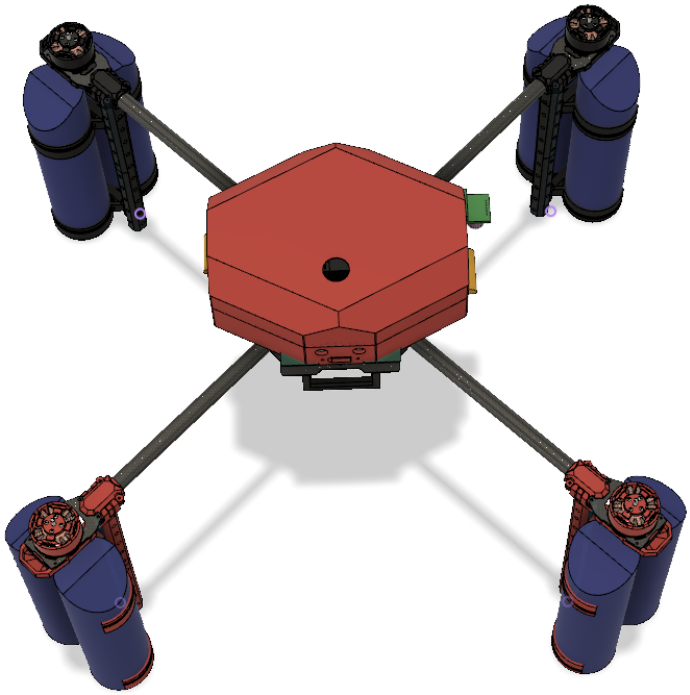

Figure 4.8: Drone design with visible ultrasound sensor.

4.1.3 Measurement of moments of inertia

In order for the drone to be available in the Gazebo simulator, a mathematical model needed to be made. As the drone is a slight modification of the base Tarot T650, which is already present in the simulator, only a few parameters would need to be tuned. These parameters were mass and moments of inertia.

The drone was weighed on a scale with an accuracy of 1 gram. The drone weighs 4903 grams with battery and 3795 grams without battery.

Moments of inertia were measured using the bifilar pendulum method along all three axes and are presented in tables 4.1, 4.2 and 4.3, and the final calculated values are presented in the table 4.4. The axes can be seen in the picture 4.10, the X axis points „forward“ between the carbon arms with black motor holders, the y axis points to the left and the z axis points upwards. In this method, the drone is hung on two filars (ropes) of known length and allowed to rest in mechanical equilibrium. Then, the drone is rotated along the axis, along which the moment of inertia is measured and when the drone is let go, it starts oscillating.

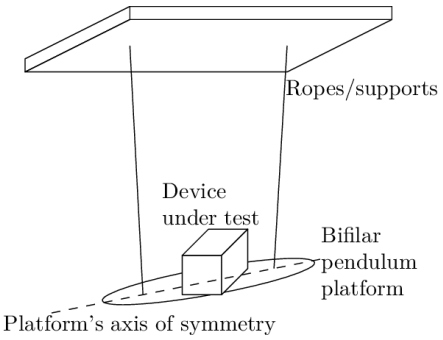

Figure 4.9: Visualisation of the bifilar pendulum method. [14]

Figure 4.10: Visualisation of the x, y and z axes for the bifilar pendulum method.

According to [15], moment of inertia can be calculated as

$$I = \frac{mgd^2}{4L\omega^2}, \tag{4.1}$$

Where m is the mass of the aircraft, g is the acceleration due to gravity, d is the distance between the filars, L is the length of the filars and ω is the angular frequency of oscillations. ω will be calculated from the period T of the oscillations as

$$\omega = \frac{2\pi}{T}. \tag{4.2}$$

The equation (4.1) can be rewritten as

$$I = \frac{mgd^2T^2}{16L\pi^2}, \tag{4.3}$$

Thus, in order to calculate I, variables d, T and L will be measured. The time was measured by a stopwatch app on a smartphone, which was

operated by a person and the lengths were measured by a tape measure. The inaccuracies and errors introduced by measurement affect the calculated inertias, nevertheless, controllers are designed to be robust and tolerate slight differences in the model and still be capable of stable flight.

No.	N of periods[-]	time[s]	T[s]	d[m]	L[m]
1	15	26.13±0.4	1.74±0.03	0.34±0.01	0.95±0.01
2	17	30.46±0.4	1.79±0.02	0.34±0.01	0.95±0.01
3	18	32.28±0.4	1.79±0.02	0.34±0.01	0.95±0.01
Avg			1.78	0.34	0.95

Table 4.1: Measurement along X axis

No.	N of periods[-]	t[s]	T[s]	d[m]	L[m]
1	15	27.34±0.4	1.82±0.03	0.34±0.01	0.95±0.01
2	15	27.17±0.4	1.81±0.03	0.34±0.01	0.95±0.01
3	15	27.08±0.4	1.81±0.03	0.34±0.01	0.95±0.01
Avg			1.81	0.34	0.95

Table 4.2: Measurement along Y axis

No.	N of periods[-]	time[s]	T[s]	d[m]	L[m]
1	15	21.98±0.4	1.47±0.03	0.34±0.01	0.95±0.01
2	19	27.89±0.4	1.47±0.02	0.34±0.01	0.95±0.01
3	20	29.26±0.4	1.46±0.02	0.34±0.01	0.95±0.01
4	25	36.55±0.4	1.46±0.02	0.34±0.01	0.95±0.01
Avg			1.47	0.34	0.95

Table 4.3: Measurement along Z axis

The calculated moments are presented in the table 4.4 and the application of this measurement is discussed in chapter 10.

Axis	Moment of inertia[kg.m^2]
X	0.1174
Y	0.1214
Z	0.1732

Table 4.4: Results of the measurement

4.2 Protective coatings

As it was previously stated in section 2.1, when water comes into contact with an electrical circuit, new conductive paths are introduced and the circuit may malfunction. To alleviate this issue, chemical surface coats are used. In this subsection, the efficacy of three various products is explored. The products are namely PVB Varnish, Plastik 70, which are protective and Fluid 101, which is a water-displacing product.

4.2.1 Testing circuit

The electrical circuit chosen for this testing was a simple astable multivibrator using the well-known 555 timer and a light emitting diode(LED) connected to its output. The schematic can be seen in the picture 8.1. This circuit is easy to diagnose, whether it is working or not, indicated by the LED.

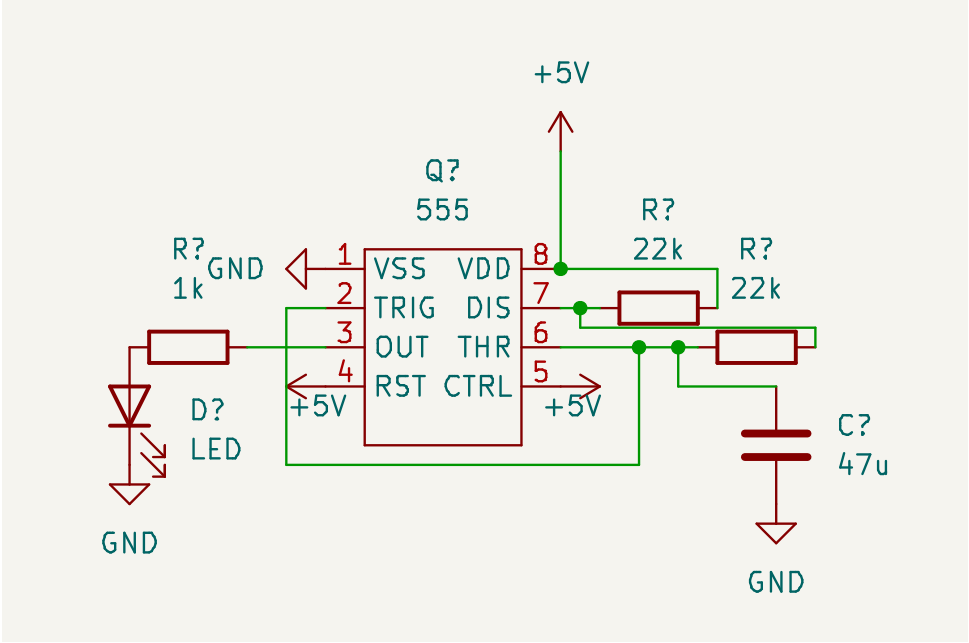

Figure 4.11: Schematic of the testing circuit.

4.2.2 Selected components

As the payload of the drone changes with every application, the water-resistivity of only a few components will be discussed.

Motors

The motors on this drone are outrunner sensorless brushless DC motors. They consist of permanent magnets on the rotor and copper coils on the stator. The copper coils are already insulated, thus no more waterproofing is required,

only the insulation around electrical connections needs to be watertight. This is ensured by using heatshrink insulation.

Printed circuit boards

Assembled printed circuit board contain exposed conductive pads. As it was stated in chapter 4, water almost always contains impurities, which are responsible for the risk of electric shorts. To prevent the shorts from forming, the circuit board needs to be coated with a waterproof coating. Such coatings are discussed in section 4.

Ultrasonic sensors

Ultrasonic sensors can be made more water resistant as an ordinary PCB. However, signal from the ultrasonic transmitter and receiver must not be too attenuated. Wrapping the transmitter and receiver with a 10μm thick plastic foil made measuring the distance impossible, thus, the receiver and transmitter will remain vulnerable to water.

Electronic speed controller (ESC)

ESCs can be made water-resistant in the same way as an ordinary PCB. However, heat output of the motor-driving transistors needs to be taken into consideration. As the used ESCs are not being utilised to their limits and the duration of experiments is short, overheating is considered not to be an issue.

Battery

The batteries themselves are often almost waterproof, the only problematic elements are the connectors. The plastic connectors will be covered with two-part epoxy glue, to close any holes in their design. When the battery is connected to the drone, the connectors fit tightly. Placing the battery above the carbon plates was considered, but this configuration is not used, as the center of gravity would shift upwards, which could cause stability issues.

4.2.3 Inadequate or insufficient waterproofing practices

One of the ideas to create a waterproof barrier is to surround the component with „hot glue “ and while the glue is hot, heatshrink tube is shrunk around the component. Hot glue is not manufactured for this purpose and wetting contact with all surfaces and materials can not be guaranteed. Thus, when the environment changes, the glue can absorb moisture or expand or shrink due to pressure, resulting in separation from the component. Even separation of 1μm will result in water flow, because the water molecules are smaller than 1 nanometre and capillary action will support the influx of water.

Chapter 5

Landing gear

In order for the drone to be able to land and float on the surface of water, specialised landing gear offering sufficient buoyancy needs to be designed and assembled. The gravitational force acting on the drone must be counterbalanced by buoyant force. For the sake of simplicity, let the component ensuring buoyancy be called a *floater*.

The MRS team commonly uses custom 3D printed landing legs. When a drone crashes, oftentimes the landing legs get broken and 3D printing is a cheap and convenient way of replacing them. The legs are designed to be a weak point, so nothing more critical gets broken. In addition, the legs have mounting holes with MRS-standardised spacing for mounting various appliances. An addition to this system is proposed - a holder for floaters.

Various floaters are considered - carbon-fibre bodies filled with foam, air-filled plastic water bottles and polyethylene foam cylinders sold as well-known „pool noodles“.

The density of used material is a good indicator, how effective the material could be as a floater. When a floater consists of more than one material, average density of its parts can be used instead. Average density can be defined as

$$\rho_a = \sum_{i=0}^{n} \frac{m_i}{V_i}, \tag{5.1}$$

where m_i is the mass and V_i is the volume of the i-th component. As the drone consists of carbon fibre and metal, its average density is larger than the density of water, thus the drone sinks, when it is introduced to a deep body of water. As a result, the average density of the floater needs to be considerably lower than the density of water.

5.1 Considered floaters

Air-filled plastic bottles

Air-filled plastic bottles have the lowest density of all considered floaters, as they consist of polyethylene tetraphtalate(PET) plastic and air.

The mass of a two-litre bottle was measured to be 54 grams. Let us approximate the volume of air is to be two litres. According to [16], the

average air density at sea level is 1.225 kg m^{-3}, thus the air weighs 2.5 grams. Therefore, the average density of such floater is approximately 30 grams per liter.

The bottles are easily available, only a reliable holder would need to be designed. However, the use of plastic bottles in this work was ruled out, as they were considered inadequate.

PE foam floaters

The floaters will be affixed to the drone using 3D printed fixtures. The fixtures will designed in such a way, that two pool noodles can be affixed to one leg, and the fixtures will be arranged, that the pool noodles are affixed to the drone on both ends. In addition, the fixtures will be easily attachable to almost all existing MRS drones, as there will be mounting holes compatible with those already mentioned in this chapter.

5.1.1 Proposed solution

The drone will have landing legs approximately 30 centimetres long and there will be two fixtures for pool noodles on each leg. The design can be seen in pictures 4.3 and 4.4. To sum up, there will be 8 cylindrical pool noodles with diameter 6.5 cm and 26 cm in length.

The complete assembly weighs approximately 170 grams and its volume is estimated by the CAD software to be 1800 cubic centimetres. Thus, the average density of this design is approximately 95 grams per liter.

Let us presume, that the drone weighs 5kg, which is its maximum take-off weight. Then the length l of submerged noodles can be calculated using

$$m = \rho V \tag{5.2a}$$

$$V = n\pi r^2 l \tag{5.2b}$$

$$l = \frac{m}{\rho n \pi r^2} = \frac{5}{1000 \cdot 8 \cdot \pi \cdot 0.0325^2} \approx 18.8\text{cm}, \tag{5.2c}$$

where m is the mass of the drone, ρ is the density of fresh water, V is the volume of displaced water, n is the number of floaters and r is the radius of floaters. This means, that in this scenario, the drone will float approximately 8 centimetres above the water surface, when at rest. As the floaters are positioned strategically, the UAV should be stable while floating.

Chapter 6

Sensors

A sensor is a device, which measures a physical quantity and outputs information about the quantity. In this chapter, various sensory options will be explored.

Experiments were carried out with three different types of sensors - a lidar, a RGB camera and two ultrasonic distance sensors. The experiments consisted of aiming the sensors at the water surface at different heights and angles and then interpreting the data received from the sensors.

6.1 Lidar RPLidar A3

The lidar is a time-of-flight sensor. This sensor emits very narrow rays of light, then captures reflected rays and measures the time difference. Using the speed of light c and time difference Δt, it is possible to calculate the distance d from the object by calculating

$$d = \frac{1}{2} c \Delta t \tag{6.1}$$

In order for this sensor to detect an object, the light rays, which were sent, must also return into the sensor. If a light ray is perpendicular to the water surface, only a fraction of the intensity of the ray is reflected back and is not detected by the sensor. The rest of the ray propagates inside the body of water and either dissipates or does not return in the time window in which the sensor expects a returning ray. If a light ray is not perpendicular to a surface, the reflected ray will not return to its origin. It is impossible for the drone to stay perpendicular to the water surface. Either way, this sensor can not be used to reliably estimate the height of the drone. It was experimentally confirmed, that the RPLidar A3 was unable to detect and report the water surface. However, it was discovered, that it has the ability to „see“ through the water and report the bottom of a shallow water body.

6.2 mvBlueFOX RGB camera

This camera is an industrial RGB camera, which can see the water surface. Unfortunately, using only taken pictures, it is impossible to estimate the

height of the camera above the surface without using items of known size.

6.3 Intel Realsense D435 RGBD camera

This camera uses active stereography to measure the depth in the captured picture. One infrared emitter and two infrared cameras are used. The cameras are oriented in the same direction and are spaced 50 millimetres apart[17]. Each camera captures the image, parts of the picture corresponding to the same elements are found and paired, the distance is calculated using trigonometry. Unfortunately, this sensor encounters the same problems as the lidar described above, as it requires a returning ray of light produced by the emitter to function properly.

6.4 Ultrasound sensors

This sensor is also a time-of-flight sensor and follows the same principle as the lidar described in 6.1. However, this sensor emits cone-shaped mechanical (sound) waves, which reflect off of the water surface well, then recaptures them and measures the time difference between these two events. According to tests, only the ultrasound sensors were able to estimate the distance to the water.

The distance is calculated in the same manner as is seen in the equation (6.1), but the speed of sound depends on environment variables, such as ambient air temperature, humidity and pressure. This sensor module contains auto-calibrating components and algorithms and the user is not expected to calibrate the sensor themselves.

Grove Ultrasonic Ranger

This module is popular among robotic hobbyists. It offers adequate performance for a low price.

Maxbotix MB1340

This sensor is industrial-grade and according to the datasheet [18] offers a high mean time between failures (MTBF), which is critical for the long-term reliability of the drone. It offers output in analog voltage, pulse-width modulation and serial communication. The last form will be used, as it is the least susceptible to noise. In addition, the sensor automatically outputs the measured distance on the serial output at the rate of 10Hz in the format `R<n><n><n>\r`, where `<n>` is a digit. It must be noted, that the sensor uses inverted serial communication, thus the meaning of the logic levels is flipped, including the start bit edge. By default, the configuration of the serial communication is the baud rate of 9600, no parity bits, one stop bit and no flow control.

6.5 PX4 autopilot internal barometer MS5611

This sensor measures the ambient air pressure and determines the height from the differences of pressure on the ground and in the position the drone currently is. However, this method does not provide the actual height above any obstacles or water surfaces. This sensor will be used to approximately measure the height of the drone above the water, when it is too high and the ultrasound sensor does not provide any measurements. In addition, if the water surface is in a different altitude than the point, from which the drone had taken off, the drone must at first land on the water, measure the ambient air pressure and use the result of this measurement as the reference for estimating its height.

Chapter 7

Sensor integration

In this chapter the integration of the chosen sensory equipment with the MRS system is described. The Robot Operating System node is developed in C++ programming language.

7.1 Robot Operating System

Robot Operating System (ROS) is a popular open-source middle ware tool for developing robots. Its main purpose is to simplify sharing information between various components of robots. It provides an environment similar to an operating system, including hardware abstraction, low-level device control, implementation of commonly-used functionality, message-passing between processes, and package management [19].

The main components of ROS are `messages`, `nodes` and `topics`. A node is an executable piece of code, essentially a program, which runs in its own thread. A message is a data structure, which gets serialised and published on a topic by a node. A topic can be viewed as a named pipe, in which nodes can write - `publish` to, or read from - `subscribe` to. Publishing the message is not reliable communication, as when a node publishes a message to a topic, it does not get any information, if any other node is subscribes to that topic and reads the message. If reliability is required, communication can be made reliable using `services`. Using the `rosrecord -a` command, one can record all topics with published messages and timestamps into a `rosbag`. The rosbag can be later analysed using `rosbag play`, which will replay the contents and the user can watch the experiment unfold the same way as it was conducted, or it can be stepped through in time steps, similarly to an old VHS tape. There also exist Python libraries for work with the rosbag as a file, freeing the user from having to play through the file.

7.2 MRS UAV System

MRS uses ROS 1 extensively in its scientific endeavours. Based on ROS, a whole system was developed by MRS, which is used both in simulations and real-world experiments. The system was developed in such a way, that

simulations would be as close to the real world as possible, as the software, which will be used in the experiments, is at first developed and tuned in the simulations, and only after that the same software is deployed on real, physical drones. This approach requires systems modeled with great attention to detail to drone and environment models, but in turn, simplifies the final real-world testing.

7.3 Sensor setup

The Maxbotix MB1340 is mounted on the outside of the shell. Signal wires go through the mini-shell inside the shell, connect to an Arduino, which is connected via USB to the Intel NUC computer.

Usually, the MRS drones are equipped with various sensors. Each sensor measures according to its frame of reference, which is often physically inside the sensor. There is a central frame of reference in the drone, and it is located in the middle of the Pixhawk. When a new sensor is mounted, a transformation in the three-dimensional Special Euclidean group, which transforms from the frame of reference of the sensor into the central frame of reference needs to be computed. Such transformation is a four-by-four matrix. Let us introduce a new frame of reference called *cermaiv2_bp* frame. The output of the sensor is a scalar value and let us define, that it lies on the x-axis of the *cermaiv2_bp* frame. It is true, that the sensor measured distance to the closest object in a cone and not in a line, however, addressing this issue is beyond the scope of this work, as the drone is meant to fly over flat water surface and in stabilised mode, so the drone is almost always perpendicular to the water surface. The transformation matrix $\mathbf{T}^{\text{central}}_{\text{cermaiv2\_bp}}$ is

$$T^{\text{central}}_{\text{cermaiv2\_bp}} = 0.001 \cdot \begin{bmatrix} 0 & 0 & -1 & 45 \\ 0 & 1 & 0 & -135.7 \\ 1 & 0 & 0 & 13 \\ 0 & 0 & 0 & 1 \end{bmatrix}. \tag{7.1}$$

For clarity, the numbers in the matrix are presented in millimetres and the coefficient in front of the matrix scales the whole matrix, as the default unit of length is the metre.

7.4 mrs_llcp package

As the MRS team continually experiments with various sensors and low-level devices, such as STM32-based modules, a unified way of interfacing these devices to the MRS ROS system was needed. Thus, the `mrs_llcp_ros` package was created. When launched, a node `$UAV_NAME/llcp` is created, which creates two topics, `/$UAV_NAME/llcp/received_message` and `/$UAV_NAME/llcp/send_message`, which are described below. The prefix $UAV_NAME can bbe specified in the MRS system, for testing it is possible to set it to `uav1`.

`/$UAV_NAME/llcp/received_message` - received messages from the low-level device are published on this topic. Other nodes can subscribe to this topic. The node listens to serial communication and publishes identical messages byte-by-byte to a topic. By default, the node opens the `\dev\arduino` device and expects serial communication with specific profile - baudrate 115200, 8 data bits, 1 stop bit, no parity, no flow control.

7.4.1 Proposed sensor integration

Connection

Usually, there is no `\dev\arduino` device, and the device connects as a `\dev\ttyUSB<n>` device, where `<n>` is a number, which can vary everytime the device is plugged in.

Both manual and automatic workarounds exist. Either the user can manually create a symbolic link by executing

```
ln -s \dev\arduino \dev\ttyUSB0
```

or can create a rule, which creates similiar symlink automatically by adding a text file to `\etc\udev\rules\`. By adding a rule defined in a text file, the addition of the symlink happens automatically and is triggered by connecting a device with the correct ID. Every USB device has specific IDs, which can be found by executing `lsusb` in the terminal and interpreting the output. It was observed, that many off-brand Arduino clones share the same IDs, thus this rule should work almost always. The used rule is listed below and when in use, it should consist of precisely one line.

```
SUBSYSTEM=="tty", ATTRS{idVendor}=="1a86",
ATTRS{idProduct}=="7524", SYMLINK+="arduino",
OWNER="mrs",MODE="0666"
```

Integration

In order to start reading measurements from the sensor, initial configuration is needed. Manual steps for the start are listed below and can be integrated into a launch script, which executes every time a drone starts.

```
roscore
roslaunch mrs_llcp_ros llcp.launch
rosrun myp llcp_listener
```

The myp package is one of the attachments to this thesis.

Chapter 8

Experiments

In this chapter, experiments, which were carried out during the work on this thesis, are described.

8.1 Waterproof protection of PCB surface

The circuit was assembled and soldered on one-sided FR1 board using THT components. Then the tested chemicals were applied by spray, then brushed in the circuit with a painting brush, then sprayed again and finally left to dry or cure. The assembled circuit can be seen in the picture 8.1.

Results

PVB Varnish. The chemical dried for 30 minutes and then the circuit was submerged in water. However, the diode stopped blinking, which means the protection was insufficient. Overall, five layers were applied in the same way and the circuit was tested after each layer. Against all expectations, this product cold not protect the circuit sufficiently.

Plastik 70. This product is similiar to PVB Varnish, but is more viscous when applied. As a consequence, the applied layer is thicker. This product worked after applying three layers and the LED blinked correctly.

Fluid 101. Fluid 101 is advertised to displace water in an already wet circuit. Unprotected testing circuit was submerged in water and subsequently the LED stopped blinking. After moving the circuit outside water, it was thoroughly sprayed with the product and the LED started blinking with the correct frequency. The product left an oily finish on the surface of the PCB. When the circuit was submerged again, it was still working correctly, but after being submerged for the third time within one minute, the circuit stopped working and oily residue was observed on the water surface. Thus, the immediate water-displacing effect was observed, but the longevity of the protective film was not impressive.

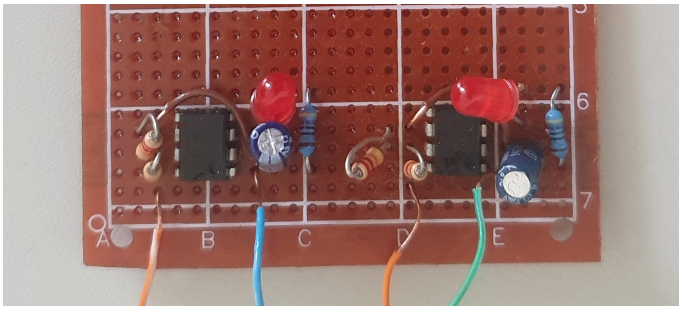

Figure 8.1: Assembled testing circuit.

8.2 Sensor performance evaluation

In order to select the optimal sensor for surface ranging, various sensors were tested, whether they can detect the water surface. The tests were conducted on the Vltava river, near Palackého square, as the place allows easy access to relatively deep water.

RpLidar A3. The sensor was operated using ROS by executing the command

```
roslaunch rplidar_ros view_rplidar_a3.launch
```

This command launches Rviz for easy visualisation. Two tests were carried out. During the first test, the sensor was aimed at concrete floor approximately one metre above ground and the output can be seen in the picture 8.2. During the second test, the sensor placed approximately 120 centimetres above water and was perpendicular to the surface. It needs to be noted, that the axis of rotation of the sensor was perpendicular to the embankment, which meant that the sensor was facing only the water or the sky. The output can be seen in the picture 8.3. The results were interpreted such as the sensor is unable to detect the surface and all rays sent by the sensor either reflect elsewhere or are absorbed.

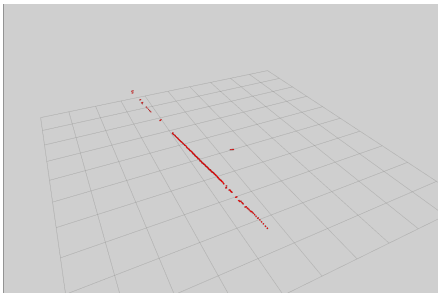

Figure 8.2: Lidar output when pointed at the ground

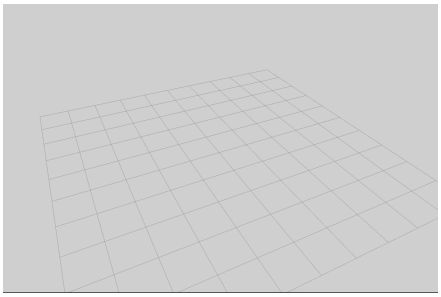

Figure 8.3: Lidar output when pointed at the water

Bluefox RGB camera. Pictures 8.4a, 8.4b and 8.4c were taken 30, 70 and 160 centimetres above the water surface. As it was expected, without knowing the parameters of the camera and the size of an object on the water surface, it is impossible to estimate the height of the drone above water.

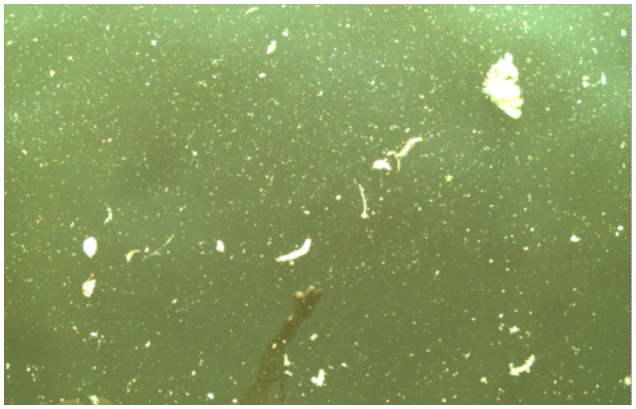

(a) : 30 centimetres above water.

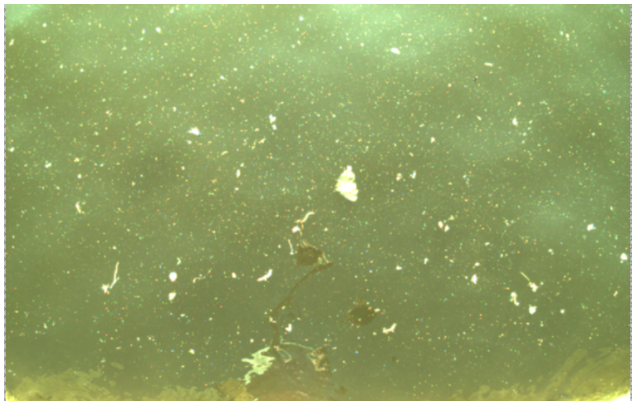

(b) : 70 centimetres above water.

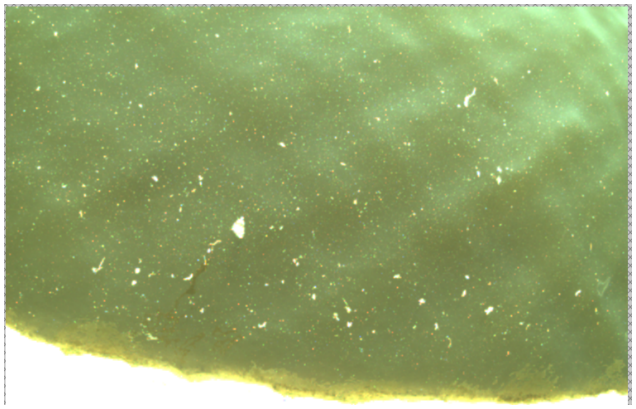

(c) : 120 centimetres above water.

Figure 8.4: Pictures from the BlueFox camera.

Grove Ultrasonic Ranger. The sensor was aimed at the water surface, the output was recorded and can be seen in the graph 8.5. The test consisted of different phases, when the sensor was situated in various heights.

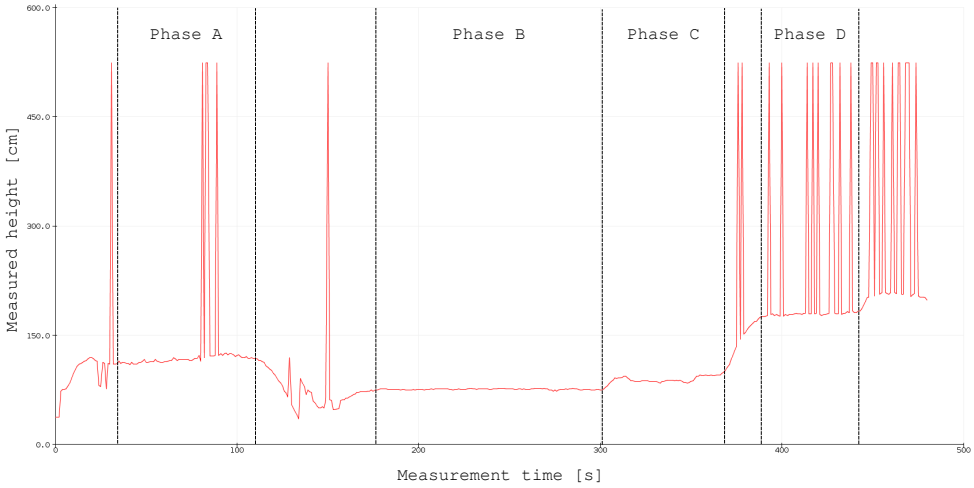

Figure 8.5: Output of the Grove Ultrasound sensor.

8.3 Floating on water

A fully equipped drone was gently put on the surface of the water. It stood afloat and when it was disturbed, it did not roll over and remained operational. However, it was noticed, that the center of gravity was not exactly in the middle, thus the drone leaned to one side. Nevertheless, it floated successfully, as it can be seen in the picture 8.6. The drone also successfully took off of the water surface. During the first takeoff, one motor spun in the incorrect direction and pushed itself and a part of the drone underwater. The drone and all its electronics survived.

Figure 8.6: Drone freely floating on the surface of water.

8.4 Flight above water

The sensor was mounted on the lower part of the top shell for ease of access with wires. A test flight was conducted and data from the sensor and Garmin Lidar-Lite was recorded. Raw data can be seen in the graph 8.7. Unfortunately, the data was not representative of reality and the sensor needed to be mounted elsewhere, as the shell was probably an obstacle for the returning sound waves. Due to time constraints of the MRS experimental campaign, no additional experiments were not carried out.

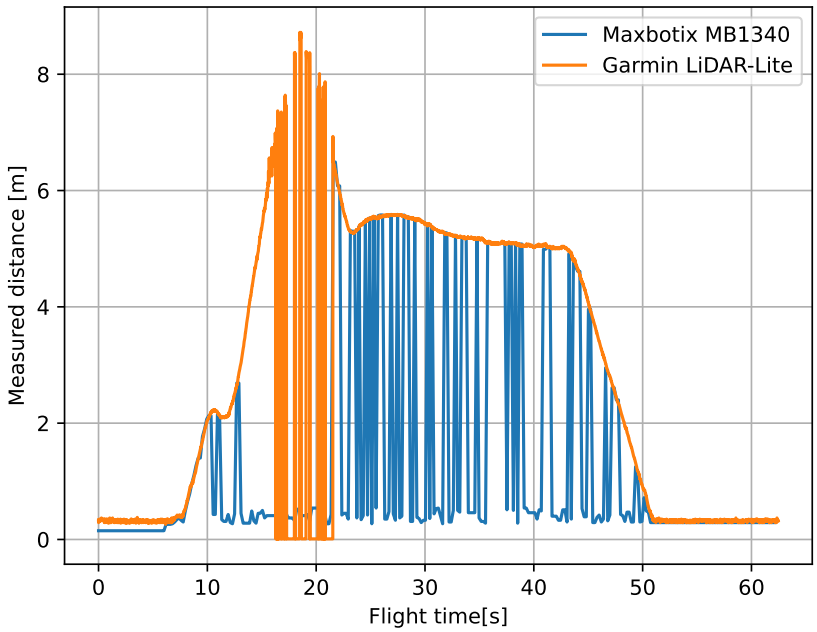

Figure 8.7: Comparison of measured data.

Chapter 9

Conclusion

A water-resistant drone with estimated IPX4 rating was designed and constructed.

The drone was also equipped with flotation devices, which ensure enough buoyancy, so that the drone can safely float on water, while all critical electronic components are in a safe distance from water. Two designs of such flotation devices were considered, one easily available and adaptable for various experiments for the MRS group, the other one was disqualified. Moments of inertia along all three axes were measured with the bifilar pendulum method and are used as parameters in MRS simulations.

Various types of sensors for the measurement of height above the water surface were considered and it was experimentally verified, that ultrasonic time-of-flight sensors are optimal. Maxbotix MB1340 ultrasonic range sensor was integrated in the MRS UAV platform, using an Arduino as a low-level device and MRS ROS llcp package as a middle-man between the Arduino and ROS system.

Chapter 10

Discussion and further work

10.1 Discussion

The final drone weighs 4903 grams. According to [12], the maximum total weight of the drone can be 5 kilograms, which means almost no additional payload can be mounted on the drone. Considering the elements added in this work, the shell contributes to the weight the most and could be made lighter by reducing the wall thickness from 4 millimetres to 3 millimetres.

The procedure of closing the shell is rather cumbersome and takes a non-trivial amount of time. The main problem is cable management, as the cables, which connect the NUC to the sensors, often collide with the air ducts and as a result, the shell can not close. Having a clear shell could improve the situation.

The measured inertias and mass were used by Bc. Ondřej Procházka in his upcoming master's thesis concerning model predictive control. Before the measurement, only an estimate of moments of inertia were used, for example the shell was approximated to be a cylinder and the estimate was larger by approximately 30%. As a consequence, the controller made control actions more intensive than required, thus the drone control was too aggressive. After the computed moments were implemented, the behaviour of the drone improved.

A new design of motor connection was implemented, which performs just as well as the old design but is more modular. However, there are three wires inside the carbon arm, which carry three-phase power to the motors. This approach could increase the level of electro-magnetic noise, thus potentially decrease the accuracy of the onboard Pixhawk GPS module or decrease the operational range of control with a radio controller.

After the experiment with the RpLidar A3, it was thought, that the Garmin Lidar-Lite will also not be able to distinguish the water surface from air, as both sensors are working on the same principle and similar wavelengths. The last experiment proved this idea wrong, as the Lidar-Lite was able to measure the distance to the water surface, although the measurement were not completely reliable. The suface of the water was calm during the experiment, which could be the reason why the optical sensor worked.

10.2 Further work

The developed drone is estimated to be IPX4 water-resistant and further work could improve its performance.

Firstly, the cooling solution for the onboard Intel NUC computer could be improved. Currently, the cooling ducts create opening in the shell, through which water can get easily inside. The redesign would include a bigger heatsink on the CPU die, which would protrude outside from the shell. The gap between the heatsink and the cut-out in the shell would be filed with silicone. The drone motors create enough airflow to cool the heatsink. This option was not explored, for it was deemed too complicated and it would not be easily replicable for a small-series assembly for a swarm for future MRS projects.

Secondly, every time the drone is moved to a different location, or when the shell is disassembled and reassembled, the Pixhawk needs to be calibrated. The reason is that the Pixhawk GPS unit moves relatively to the Pixhawk board, which could affect the ability of the controller to control the drone. To be specific, the process consists of accelerometer and magnetometer calibration. Currently, a micro-USB cable connection from a computer to the Pixhawk is needed. The calibration process is rather unwieldy and requires two people. It is possible to calibrate the Pixhawk wirelessly, using radios, which support the SiK protocol. The protocol is open-source and is maintained by a github user LorenzMeier. A specific SiK product called Holybro Telemetry Radio exists, which connects to the TELEM1 port of the Pixhawk and replaces the wired connection.

Another proposed design for floaters uses carbon-fibre floater filled with foam. Thesis supervisor Ing. Stoudek designed these floaters and further experiments will be carried out using these. When compared, the carbon floaters are more durable but heavier and their narrower design allows the drone to oscillate more when floating.

Finally, the design of the shell could be improved. Instead of connecting the sensors directly to the NUC and having to simultaneously manage many cables, a USB hub could improve this situation. In addition, the shell would consist of three parts - the bottom part would stay the same, the new middle part would have the same function as the old top part combined with the bottom part of the mini-shell, and the new top part would fit on the middle part and would allow the sensor cables to exit the shell is the same manner as is implemented in the mini-shell. The USB hub would reside in the compartment created by the new middle and top parts. This idea was not realised, because the idea was stumbled upon six days before the deadline.

Bibliography

[1] SARTORIUS GmbH.. *Resistivity Measurement of Purified Water*. 2022. Accesible on: https://www.labmanager.com/white-papers-and-application-notes/resistivity-conductivity-measurement-of-purified-water-19691. "Accessed: 28.4.2022".

[2] ZHENG Zeyu, Yang FU, Kaizhou LIU, Rui XIAO, Xiaohui WANG a Haibo SHI. Three-stage vertical distribution of seawater conductivity. Scientific Reports. 2018, 8(1). ISSN 2045-2322. Accessible on: doi:10.1038/s41598-018-27931-y.

[3] International Electrotechnical Commission. IEC 60529. https://webstore.iec.ch/preview/info_iec60529%7Bed2.1%7Db.pdf, 2001. Accessed: 28.4.2022.

[4] ŠTANC Daniel. Design of a robotic water sampler for an unmanned aerial vehicle. https://dspace.cvut.cz/handle/10467/99178, 2021. Accessed: 30.4.2022.

[5] BAI, Yiyun, Ju-Hyeon HONG a Argyrios ZOLOTAS. Development of a Novel Water Landing UAV with Deflatable Floater. 2019 Workshop on Research, Education and Development of Unmanned Aerial Systems (RED UAS). IEEE, 2019, 2019, 166-171. ISBN 978-1-7281-6600-1. Accessible on: doi:10.1109/REDUAS47371.2019.8999694.

[6] NIU, Hanlin, Ze JI, Pietro LIGUORI, Hujun YIN a Joaquin CARRASCO. Design, Integration and Sea Trials of 3D Printed Unmanned Aerial Vehicle and Unmanned Surface Vehicle for Cooperative Missions. 2021 IEEE/SICE International Symposium on System Integration (SII). IEEE, 2021, 2021-1-11, 590-591. ISBN 978-1-7281-7658-1. Accesible on: doi:10.1109/IEEECONF49454.2021.9382687.

[7] TAN, Yu Herng a Ben M. CHEN. A Lightweight Waterproof Casing for an Aquatic UAV using Rapid Prototyping. 2020 International Conference on Unmanned Aircraft Systems (ICUAS). IEEE, 2020, 2020, 1154-1161. ISBN 978-1-7281-4278-4. Accessible on: doi:10.1109/ICUAS48674.2020.9214029.

[8] XUAN-MUNG, Nguyen, Sung Kyung HONG, Ngoc Phi NGUYEN, Le Nhu Ngoc Thanh HA a Tien-Loc LE. Autonomous Quadcopter Precision Landing Onto a Heaving Platform: New Method and Experiment. IEEE Access. IEEE, 2020, 2012, 8, 167192-167202. ISBN 978-1-4673-0829-8. ISSN 2169-3536. Accessible on: doi:10.1109/ACCESS.2020.3022881.

[9] SwellPro Inc.. *SwellPro Fisherman FD1*. Accessed on: 17.5.2022. Accessible on :`https://www.swellpro.com/fisherman-fishing-drone.html`.

[10] SwellPro Inc.. *SwellPro Splash*. Accessed on: 17.5.2022. Accessible on :`https://www.swellpro.com/spry.html`.

[11] SwellPro Inc.. *SwellPro Spry+*. Accessed on: 17.5.2022. Accessible on :`https://www.swellpro.com/waterproof-splash-drone.html`.

[12] UAV systems international. Tarot 650 kit. `https://uavsystemsinternational.com/products/tarot-650-ready-to-fly-drone`, 2020. Accessed: 30.4.2022.

[13] amanusk. Terminal-based CPU stress and monitoring utility. GitHub [online]. 2021 [Accessed: 2022-05-17]. Accessible on: `https://github.com/amanusk/s-tui`.

[14] SHIPMAN, William John. *The Nonlinear Modelling and Model Predictive Control of a Miniature Helicopter UAV*. 2012. Accessed on: 15.5.2022. Accessifle on: `https://www.researchgate.net/publication/333560096_The_Nonlinear_Modelling_and_Model_Predictive_Control_of_a_Miniature_Helicopter_UAV`.

[15] HABECK, Joseph and SEILER, Peter. Moment of Inertia Estimation Using a Bifilar Pendulum. University of Minnesota. 2016. Accessed: 3.5.2022. Accessible on: `https://hdl.handle.net/11299/182514`.

[16] NATIONAL AERONAUTICS AND SPACE ADMINISTRATION. *U.S. Standard Atmosphere*. 1976. LCCN 77601158. Accessible on: `https://www.ngdc.noaa.gov/stp/space-weather/online-publications/miscellaneous/us-standard-atmosphere-1976/us-standard-atmosphere_st76-1562_noaa.pdf`. Accessed on: 20.5.2022.

[17] INTEL. Intel® RealSense™ D400 Series Product Family Datasheet. Revision 005. January 2019. [Accessed: 2022-05-18]. Accessible on: `https://www.intel.com/content/dam/support/us/en/documents/emerging-technologies/intel-realsense-technology/Intel-RealSense-D400-Series-Datasheet.pdf`.

[18] MaxBotix Inc., *XL-MaxSonar®-AE4 Datasheet*. 2009. Accessed on: 12.5.2022. Accessible on: `https://www.maxbotix.com/documents/XL-MaxSonar-EZ_Datasheet.pdf`.

[19] ROS Wiki. http://wiki.ros.org/Documentation. Accessed: 3.5.2022.